JCIM JOURNAL OF CHEMICAL INFORMATION AND MODELING

pubs.acs.org/jcim Article

Dynamics of the Histone Acetyltransferase Lysine-Rich Loop in the Catalytic Core of the CREB-Binding Protein

Ilaria Salutari and Amedeo Caflisch*

Cite This: https://doi.org/10.1021/acs.jcim.1c01423 Read Online

ACCESS | Metrics & More | Article Recommendations | Supporting Information

ABSTRACT: The tight control of transcriptional coactivators is a fundamental aspect of gene expression in cells. The regulation of the CREB-binding protein (CBP) and p300 coactivators, two paralog multidomain proteins, involves an autoinhibitory loop (AIL) of the histone acetyltransferase (HAT) domain. There is experimental evidence for the AIL engaging with the HAT binding site, thus interrupting the acetylation of histone tails or other proteins. Both CBP and p300 contain a domain of about 110 residues (called the bromodomain) that recognizes histone tails with one or more acetylated lysine side chains. Here, we investigate by molecular dynamics simulations whether the AIL of CBP (residues 1556−1618) acetylated at the side chain of Lys1595 can bind to the bromodomain. The structural instability and fast unbinding kinetics of the AIL from the bromodomain pocket suggest that the AIL is not a ligand of the bromodomain on the same protein chain. This is further supported by the absence of strong and persistent contacts at the binding interface. Furthermore, the simulations of unbinding show an initial fast detachment of the acetylated lysine and a slower phase necessary for complete AIL dissociation. We provide further evidence for the instability of the AIL intramolecular binding by comparison with a natural ligand, the histone peptide H3K56ac, which shows higher stability in the pocket.

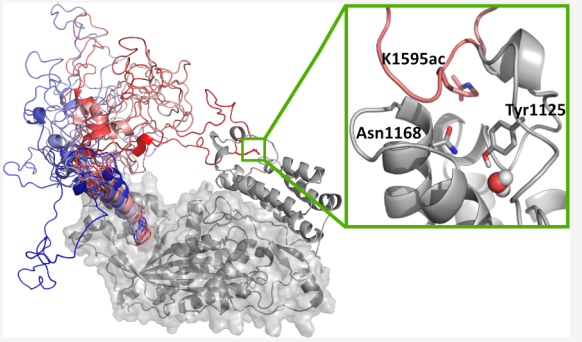

INTRODUCTION

Histone acetyltransferases (or HATs) are multidomain proteins crucial to the regulation of gene expression. Experimental evidence indicates that they cooperatively bind and coordinate the assembly of multicomponent transcription factor complexes, which include chromatin remodeling factors and proteins that realize post-translational modifications on the DNA.[1−4] The CBP/p300 proteins (or CREBBP/EP300; CREB-binding protein/E1A binding protein p300) constitute a family of HATs[5] and are considered to be a central hub in the large network of gene regulation. CBP and p300 are known to have up to 400 different interacting partners,[6] and they are localized at the regulatory region of more than 16 000 human genes.[7] To date, several studies involving gene mutations or gene knockouts of CBP/p300 have tried to shed light on the role of these proteins.[8−12] CBP and p300 share high sequence identity and structural similarity in the catalytic core. The folded functional domains of the core are the bromodomain, which binds acetylated lysines; the HAT domain, which catalyzes the acetyl transfer to substrates; and the PHD and RING domains, both of which possess regulatory functions.

Regulation of the catalytic activity of CBP/p300 has been investigated, and it often involves protein interactions with domains adjacent to the catalytic core.[13−18] Furthermore, the catalytic core itself possesses autoregulatory activity. It has been proposed that the RING domain, which is connected to the rest of the protein core by long flexible loops, can move close to the HAT catalytic site and impair substrate binding.[19,20] Evidence has accumulated for another regulatory mechanism by the lysine-rich loop of the HAT domain (also called the autoinhibitory loop, or AIL).[21] The AIL is a 63-residue-long disordered region (residues 1556−1618 in human CBP) that stems from the HAT domain (residues 1323−1700). Its primary role is to bind an electronegative patch close to the HAT catalytic site, thus blocking the entrance of substrates and further acetylation activity.[20−22] However, as discussed by Park and coworkers,[18] the lysines of the AIL could also be acetylated, making them possible ligands of the bromodomain. The authors propose that the acetylated AIL of CBP can engage the bromodomain intramolecularly and thus compete with histone ligands. The negative regulation of bromodomain activity through acetylation would allow the CBP catalytic core to detach from chromatin or other binding partners.

The bromodomain binding pocket bears the characteristics of a disordered binding site, due to the presence of flexible loops (ZA and BC loops) that connect the rigid α-helices of the

Received: November 23, 2021

https://doi.org/10.1021/acs.jcim.1c01423
J. Chem. Inf. Model. XXXX, XXX, XXX−XXX

conserved bromodomain fold. The ZA loop is longer, and it exhibits the most sequence variations and structural differences across bromodomain families.[23] In CBP, the ZA and BC loops consist of residues 1103−1135 and 1167−1172, respectively. Previous studies have employed molecular dynamics (MD) simulations to identify the conformations adopted by bromodomains in the apo state.[24−28] The results have given valuable insight into the structural flexibility of the binding site, especially of the ZA loop, which can be applied to drug discovery. Other studies have attempted to identify the preferred binding motifs of bromodomains to their substrates, e.g., either the acetylated lysine or differently acetylated histone peptides.[29−34] These studies have contributed to our understanding of which bromodomain residues are important for ligand binding, information that can be further exploited to design competitive inhibitors.[35−40]

As of now, MD simulations have not yet studied the disordered AIL as a possible substrate of the CBP bromodomain. Furthermore, there are no published crystal structures of the CBP bromodomain in complex with AIL peptides. Given the disordered nature of the AIL region and of the bromodomain binding loops, MD simulations are certainly a valuable tool to study the dynamic interplay between the two and reveal the pattern of contacts at the atomic level of detail. Two unanswered questions are whether the AIL can effectively reach the bromodomain and whether there are persistent contacts between specific residues of the AIL and residues in the binding pocket of the acetylated lysine. We have employed atomistic simulations of the CBP catalytic core to analyze the AIL dynamics and potential binding to the bromodomain on the same protein molecule. The size of the simulated system (620 residues) proves challenging in terms of computational resources, and we have used an implicit solvent model, as was done in the simulations of the AIL in the p300 catalytic core.[20]

RESULTS

We first analyze the simulations of the CBP catalytic core with the reconstructed AIL. This is followed by the results of the CBP bromodomain complexes with AIL and histone peptides. Table 1 summarizes all the simulations.

AIL Detaches from the Bromodomain in the CBP Catalytic Core. To identify whether the AIL remains bound to the bromodomain, we measure the distance between the acetyl oxygen of acetylated Lys1595 (K1595ac) and the buried structural water molecule. Lys1595 was chosen for acetylation to compare our results to the NMR data which proposed intramolecular AIL binding to the bromodomain.[18] Note that the structural water molecule is involved in hydrogen bonds with both the hydroxyl of the conserved Tyr residue (at the bottom of the pocket) and the acetyl oxygen of acetylated lysines in the crystal structures of bromodomains and histone peptides.[23,41,42]

In 20 of 36 independent runs (of 100 ns each) the AIL completely dissociates from the bromodomain pocket, reaching a distance larger than 20 Å (see Table 1 and Figure 2). In the remaining 16 runs, there are two possible binding modes, represented in Figure 1. The less populated state shows K1595ac−water distances peaked at 3 Å and can be defined as the canonical bound state, in which the K1595ac is inserted in the bromodomain pocket where it establishes the conserved interactions seen in crystal structures. Unexpectedly, there is a higher population of an intermediate state between bound and fully dissociated AIL, in which K1595ac is solvent exposed, while the AIL is still in contact with the bromodomain. The distance between K1595ac and the structural water fluctuates between 10 and 18 Å. There are numerous contacts maintained between a subset of AIL residues (including K1595ac) and the bromodomain binding loops. One persistent contact is established between K1595ac and the side chain of Leu1120 in the ZA loop (Figure 1).

Table 1. Overview of the Systems Simulated in This Study[a]

simulated system	length of each run [ns]	unbinding time[b] [ns]	AIL unbinding events	K1595ac unbinding events
whole catalytic core				
C → N backbone	100	61	20	36
bromodomain−AIL endecamer				
C → N backbone	200	268	18	22
C → N backbone	100	156	16	24
C → N backbone	100	95	22	25
bromodomain−AIL pentamer				
C → N backbone	100	70	26	31
bromodomain−flipped AIL				
N → C backbone	500	52	33	33
bromodomain−histone				
N → C backbone	500	1200	9	11

[a]The backbone N → C direction refers to the orientation of the bound acetylated lysine relative to the bromodomain pocket. Each system is simulated in 36 independent runs which differ in the random assignment of the initial velocities. The three rows in the bromodomain−AIL endecamer group include two iterations. For each iteration, 36 starting structures were chosen among the structures with acetylated Lys1595 (K1595ac) bound to the bromodomain in the previous iteration. [b]The unbinding times are calculated by the cumulative distribution function and refer to a complete detachment.

The individual time series of the K1595ac−water distance are reported in Figure 2. Almost all replicas lose the canonical bound state during the first 10 ns of the simulation. One observes either full dissociation or an intermediate state prior to the complete detachment of the AIL segment. The events of K1595ac reinsertion in the binding pocket are extremely rare (clearly visible only in replicas 19 and 21, for roughly 20 ns). These simulation results suggest that the AIL does not occupy the bromodomain pocket and thus does not compete for the binding of histone peptides.

Upon detachment of the AIL we do not observe displacement of the bromodomain with respect to the HAT domain (Figure S1). This indicates that in our model the bromodomain is not strained in its position closer to the HAT domain, when the AIL is bound. We highlight that the RING domain, which is localized approximately between the bromodomain and the HAT, is absent in the crystal structure of the CBP core[18] and in the simulated model. Although the RING domain is connected to the catalytic core by long and flexible loops, it might modulate the relative position and orientation of the bromodomain and HAT domain.

Kinetics of AIL Unbinding in the Catalytic Core. The kinetics of AIL dissociation from the bromodomain are measured with the cumulative distribution function of the unbinding times.[43] The cumulative distribution function is expressed as

$$f(t) = \int_t^\infty \rho(\tau)\, d\tau$$

https://doi.org/10.1021/acs.jcim.1c01423
J. Chem. Inf. Model. XXXX, XXX, XXX−XXX

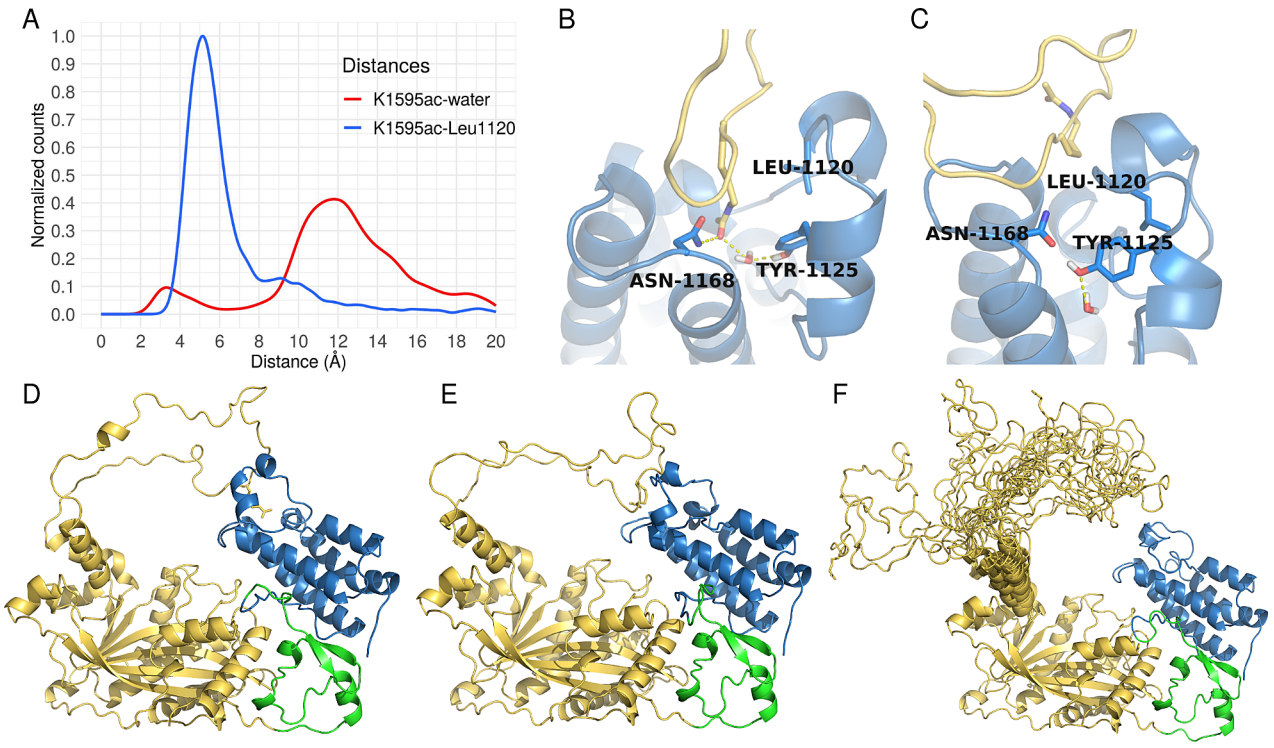

Figure 1. Metastable state in the simulations of the whole catalytic core. (A) Distribution of distances between the K1595ac and two interacting partners. The distance between the K1595ac and the water shows clearly the presence of two states, where the most populated is the intermediate bound state (between 10 and 18 Å). The K1595ac−Leu1120 distance is the center-of-mass distance between the side chains of the two residues, and the peak at 5 Å represents the intermediate bound state. Sampling of the unbound AIL state, above 20 Å, is not shown. Representative snapshots of the K1595ac (yellow, in sticks) in the (B) canonical and (C) intermediate bound states. The canonical state maintains the hydrogen bonds (yellow dashed lines) to the acetyl oxygen of the K1595ac, while the intermediate state looses the hydrogen bonds and the K1595ac is solvent exposed. Representative snapshots of the AIL in the (D) canonical bound state, (E) intermediate bound state, and (F) fully unbound AIL (overlap of 13 snapshots). In all the snapshots, the HAT domain is colored in yellow, the bromodomain is in blue, and the PHD is in green.

where ρ is the probability distribution of the unbinding times and τ represents the characteristic unbinding time obtained from fitting an exponential function. A threshold on the K1595ac acetyl oxygen distance to the structural water is used to define an unbinding event.

We use two distance thresholds to characterize the kinetics of the canonical and the intermediate bound states. A distance threshold of 30 Å represents the complete detachment of the AIL from the bromodomain. The kinetics are represented by a single-exponential fit with a characteristic unbinding time of 61 ns (Figure 3A). A more stringent threshold of 8 Å is used to identify the loss of K1595ac from the bromodomain pocket. The threshold at 8 Å takes into account the thermal fluctuations of the acetylated lysine−water distance (in Figure 1A, the histogram of the K1595ac−water distance shows the first peak until a distance of about 6 Å, which corresponds to twice the optimal hydrogen bond distance). The kinetics are represented by a single-exponential fit with a characteristic unbinding time of 2 ns (Figure 3B), which is substantially faster than the full AIL detachment. The unbinding times of the K1595ac are robust with respect to the distance threshold in a range of distances from 10 to 16 Å (Table S1). Overall, the initial bound state of the AIL is lost rapidly in all replicas of the catalytic core, while an intermediate bound state is populated in 16 of the 36 replicas.

Contacts between the AIL and the Bromodomain. To investigate the intramolecular contacts involved in binding the AIL, we have calculated the contact map of the catalytic core. The contacts are represented as two-dimensional histograms, where the frequency of contact is colored as a heat map in a linear color scale. The distance threshold to determine the presence of a contact is set at 5 Å between any pair of residue atoms. Figure 4 shows the contacts between the AIL and the bromodomain ZA and BC loops, relative to the canonical and intermediate bound states. The distinction between the canonical and intermediate states is based on the K1595ac−water distance, and the frequency of contacts is normalized between 0 and 1 for both states.

In the canonical bound state, the majority of contacts involves the stretch of bromodomain residues from Val1115 to Ile1122 in the ZA loop. The bromodomain residues in this stretch are mostly hydrophobic, and they contact K1595ac, the asparagines, and the lysines in a short region of the AIL. In the BC loop, three hydrophobic residues (Ala1164, Tyr1167, and Val11714) and the conserved Asn1168 contact K1595ac. These interactions are consistent with the contacts observed in crystal structures of the CBP bromodomain with histone peptides.[23,41,44] The intermediate state shows a small core of contacts involving hydrophobic residues on the ZA loop, while the interactions necessary for the insertion of K1595ac in the binding pocket are lost (e.g., interaction with Asn1168, Tyr1125, and Tyr1167). In both states, the aspartate triad (Asp1116, Asp1124, and Asp1127) of the ZA loop is not involved in persistent contacts with the numerous lysines of the AIL. Only Asp1124 and Lys1597 have a contact frequency of 75% in the canonical state.

To further investigate if the contacts of the AIL on the bromodomain are specific to the AIL sequence, we analyze the pattern of hydrogen bonds (H-bonds) at the interface. The H-bonds are calculated with a 4.0 Å distance cutoff between donor

https://doi.org/10.1021/acs.jcim.1c01423
J. Chem. Inf. Model. XXXX, XXX, XXX−XXX

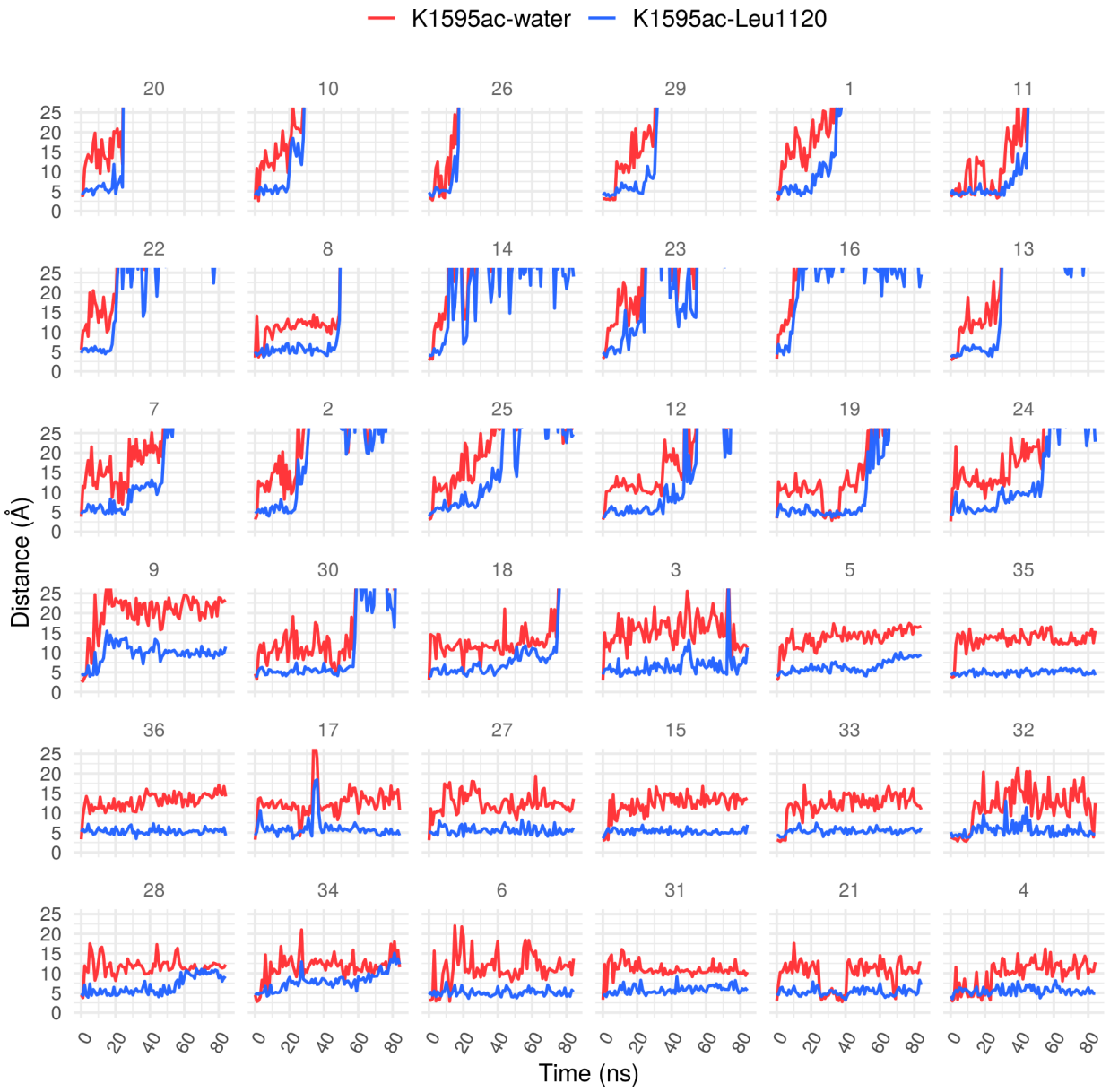

Figure 2. Temporal evolution of the AIL bound states. Time series of the K1595ac acetyl oxygen distance to the structural water (red line), and of the K1595ac side chain center-of-mass distance to the Leu1120 side chain (blue line). The replicas are placed in decreasing order of the average values of the K1595ac−water distances, calculated in the second half of each individual run. The first 20 replicas show full detachment of the AIL, while the last 16 show the AIL in the intermediate state.

(nitrogen) and acceptor (oxygen) atoms of the residues identified in the contact maps. Table 2 lists the atoms involved in H-bonds and their frequencies relative to the canonical and intermediate states. We identify H-bonds specific to the AIL sequence, which involve the AIL side chains, and H-bonds not specific to the AIL sequence, which involve the AIL backbone. Overall, the majority of H-bonds are formed between the backbone of the AIL and the backbone of the bromodomain, in both the canonical and intermediate states. They are usually present for more than half of the time spent in either the canonical or intermediate state. The sequence-specific H-bonds involving the AIL side chains are present for less than half of the time spent in each state. The only exception is the H-bond between the K1595ac acetyl oxygen and the Asn1168 side chain nitrogen, which has a frequency of 84% in the canonical state. This indicates that Asn1168 is the most relevant interaction for K1595ac insertion in the pocket, consistent with the information available from bromodomain crystal structures with histones.

We do not identify strong contacts between side chains of polar or charged residues at the interface, with the exception of the conserved Asn1168. Thus, the sequence of the AIL does not seem to be a ligand of the CBP bromodomain. For other bromodomains, it has been suggested that electrostatic interactions of the ZA loop extending into solution play a role in histone peptide recruitment.[33,45] On the other hand, the ZA loop in CBP/p300 is mainly hydrophobic, a feature that is not shared among the bromodomain families, which exhibit heterogeneous electrostatic potentials on the binding site surface.[23]

Peptides in Complex with the Bromodomain. We decided to compare our results indicating AIL unbinding with the behavior of a known peptide ligand. For this purpose we have

https://doi.org/10.1021/acs.jcim.1c01423
J. Chem. Inf. Model. XXXX, XXX, XXX−XXX

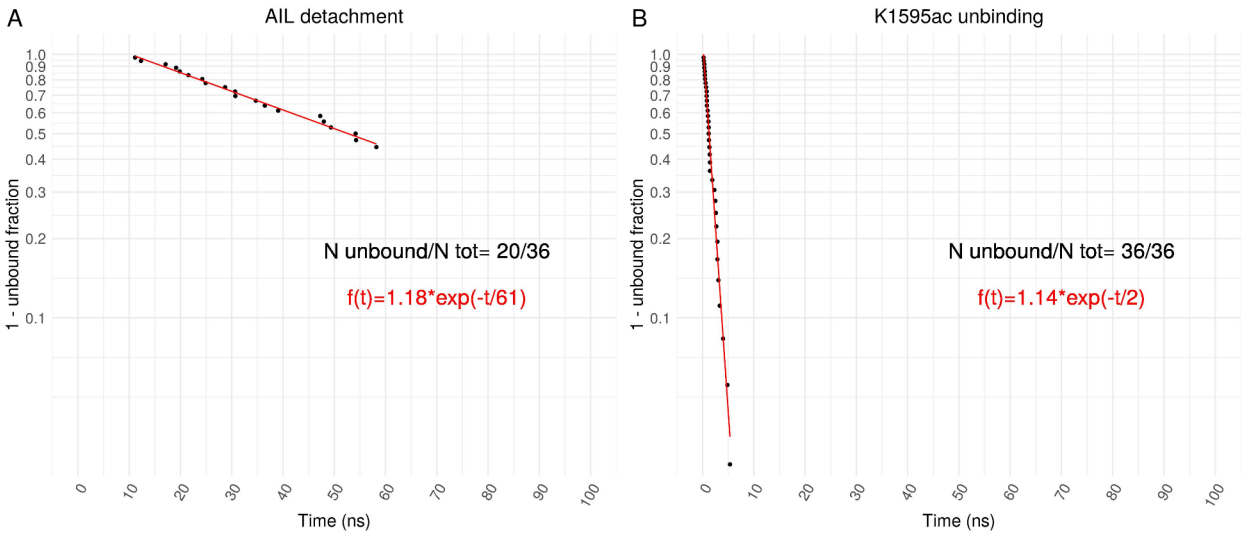

Figure 3. Kinetics of AIL unbinding. The graphs show a two-parameter exponential fit with the characteristic unbinding times (τ). The number of unbinding events is also reported ($N_{unbound}$). (A) The full detachment of the AIL has a characteristic time of 61 ns. (B) The K1595ac exits the bromodomain pocket in 2 ns. The fit with a one-parameter exponential, i.e., fixing the multiplicative constant to 1.0, yields characteristic times of 83 and 2 ns for the full detachment and exit of K1595ac from the pocket, respectively.

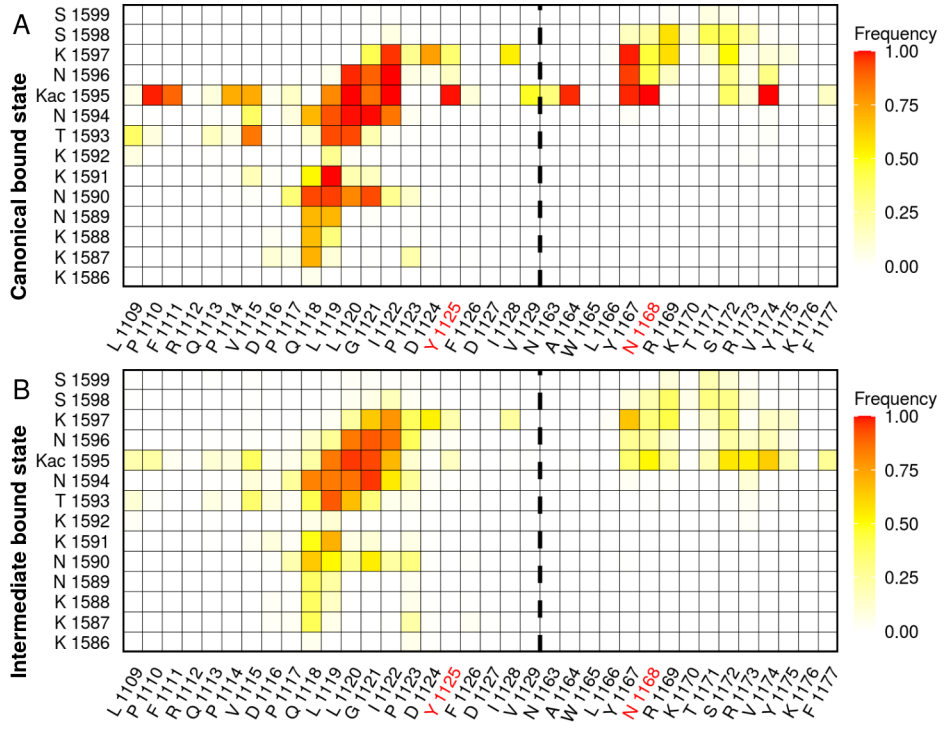

Figure 4. Map of contacts between the AIL and the bromodomain. Panels A and B include only the snapshots of the canonical bound state and intermediate bound state, respectively. The linear color scale is normalized from 0 to 1, where 0 (white) indicates no contact and 1 (red) is 100% frequency of contact. The bromodomain and AIL residues are labeled on the *x*-axis and *y*-axis, respectively. The vertical dashed line separates the ZA loop (first part) from the BC loop (second part). Highlighted in red are the conserved tyrosine and asparagine residues important for acetylated lysine binding. These contacts are lost in the intermediate state.

carried out simulations of the bromodomain in complex with the histone peptide and with different sequences of AIL peptides. Given that the histone is the natural ligand of the CBP bromodomain, it is expected to have a higher stability in the binding pocket with respect to the AIL peptides.

The bromodomain with histone peptide was prepared from a crystal structure (PDB 5GH9) with monoacetylated H3K56ac peptide, a frequent acetylation mark for CBP.[41] One residue at the N-terminal and five residues at the C-terminal were added to the histone manually by using PyMOL,[46] to have a peptide length comparable to the AIL endecamer. The sequence of the histone is IRRYQ(K56ac)STELL.

Crystal structures of the bromodomain in complex with peptides derived from the AIL sequence are not available, and we prepared two different starting models of the complex (see Table 1 for all bromodomain simulations). The sequence of the

https://doi.org/10.1021/acs.jcim.1c01423
J. Chem. Inf. Model. XXXX, XXX, XXX−XXX

Table 2. List of Hydrogen Bonds between AIL and Bromodomain Residues[a]

Nonspecific to AIL sequence					
canonical bound state			intermediate bound state		
AIL backbone	BRD backbone	freq (%)	AIL backbone	BRD backbone	freq (%)
Asn1594 N	Leu1119 O	70	Asn1594 N	Leu1119 O	54
K1595ac N	Leu1120 O	77	K1595ac N	Leu1120 O	73
Asn1596 N	Leu1120 O	62	Asn1596 N	Leu1120 O	72
–	–	–	Asn1596 N	Gly1121 O	39
canonical bound state			intermediate bound state		
AIL backbone	BRD side chain	freq (%)	AIL backbone	BRD side chain	freq (%)
Asn1590 N	Gln1118 OE1	33	–	–	–
Lys1597 N	Tyr1167 phenyl O	39	–	–	–
Specific to AIL sequence					
canonical bound state			intermediate bound state		
AIL side chain	BRD side chain	freq (%)	AIL side chain	BRD side chain	freq (%)
Lys1597 NZ	Asp1124 OD1	35	Lys1597 NZ	Asp1124 OD1	39
Lys1597 NZ	Asp1124 OD2	37	Lys1597 NZ	Asp1124 OD2	39
K1595ac acetyl N	Tyr1125 phenyl O	32	–	–	–
K1595ac acetyl O	Asn1168 ND2	84	–	–	–
canonical bound state			intermediate bound state		
AIL side chain	BRD backbone	freq (%)	AIL side chain	BRD backbone	freq (%)
Asn1590 ND2	Gln1118 O	49	Asn1594 ND2	Gln1118 O	32
Asn1594 ND2	Leu1120 O	31	–	–	–

[a]The residues selected have a contact frequency above 75% in the contact maps. The donor and acceptor atoms are the side chain and backbone nitrogens and oxygens, respectively. The frequencies (%) are normalized to the canonical and intermediate states. Only the hydrogen bonds with a frequency above 30% are listed. "BRD" is the abbreviation for bromodomain.

AIL endecamer is KKNTN(K1595ac)NKSSI. The first model is taken from the CBP catalytic core with the AIL inserted in the bromodomain. Here, the intermolecular distances are those found in the catalytic core at the start of the simulations. For this model, we have generated an AIL endecamer (simulated in two additional iterations) and an AIL pentamer, to verify the effect of peptide length. The second model uses the histone crystal structure (PDB 5GH9) and mutates the histone sequence, except for the acetylated lysine, to the AIL sequence. This model is called "flipped" AIL, due to the N → C backbone direction. Here, the position of the acetylated lysine is the same as that of the histone crystal pose. Note that the backbone N → C direction of the AIL peptide relative to the bromodomain pocket is opposite in the two starting models (all backbone directions are listed in Table 1). This does not influence the AIL peptide behavior, as both models exhibit high unbinding rates. The influence of the backbone N → C orientation of histone peptides in bromodomains has been investigated[47,48] and it was observed that crystal structures of some bromodomains may have opposite histone peptide backbone directions, without consequences to acetylated lysine binding.

AIL Peptide Detaches from the CBP Bromodomain. All of the complexes with an AIL peptide show peptide detachment in the majority of the replicas, while the histone peptide has the lowest detachment rate (Table 1). The AIL endecamer shows the highest degree of detachment in the last iteration (22 replicas out of 36). Thus, the AIL endecamer is not stable in the bromodomain pocket even after an extensive sampling of the bound state, as the last iteration starts from the bound replicas of the previous iterations. The AIL pentamer detaches more frequently (26 replicas out of 36) than the AIL endecamer, because it has fewer peptide residues interacting with the bromodomain loops. Interestingly, the "flipped" AIL complex shows the highest peptide unbinding rate (33 replicas out of 36), suggesting that its N → C direction, which is identical to that of the histone, is not favored in AIL binding.

Figure 5 shows the distributions of K1595ac to water distances for all bromodomain−peptide complexes. The histone samples the canonical bound state more than all other peptides. All peptides show almost no occurrence of the intermediate state

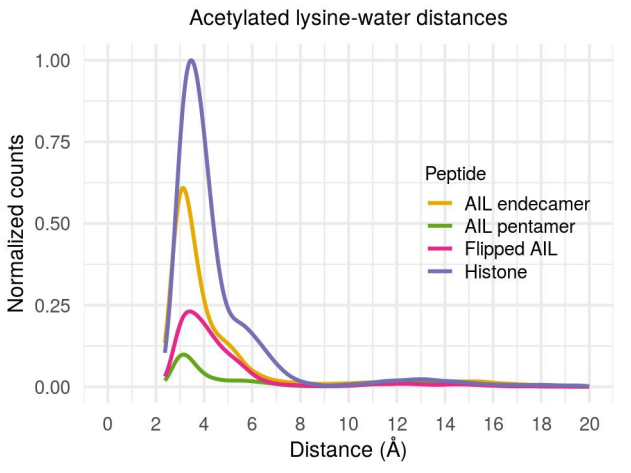

Figure 5. Simulations of bromodomain/peptide complexes. Distribution of acetylated lysine (acetyl oxygen) distances to structural water. The AIL endecamer iterations are pooled in the same distribution. The intermediate state (between 10 and 18 Å) is populated only negligibly as the peptides fully dissociate rapidly upon exit of K1595ac from the pocket. Sampling of the unbound peptide (distances higher than 20 Å) is not shown. The complexes have different simulation lengths. The counts for each system are normalized with respect to the peak of the histogram of the histone peptide.

https://doi.org/10.1021/acs.jcim.1c01423
J. Chem. Inf. Model. XXXX, XXX, XXX−XXX

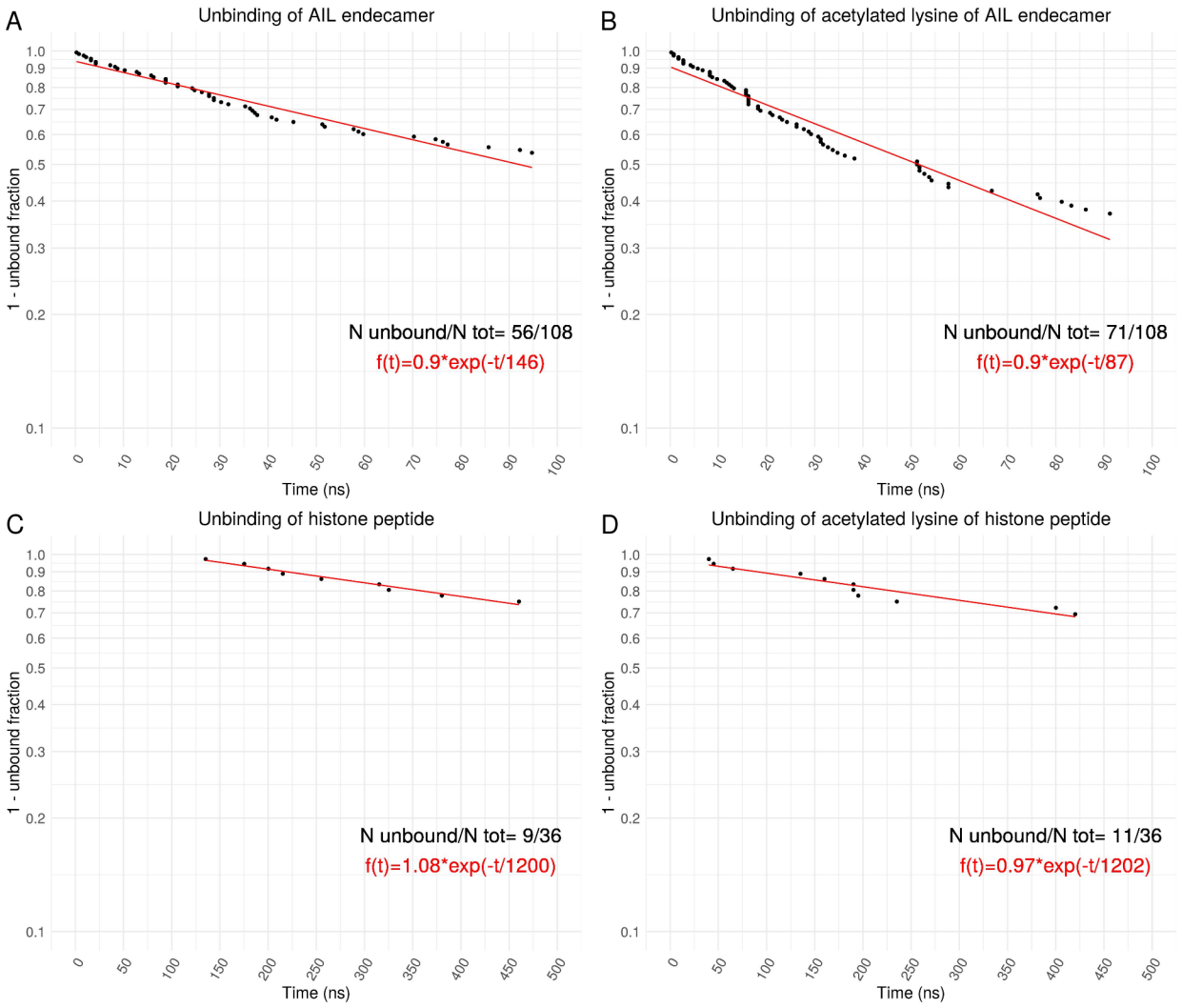

Figure 6. Unbinding kinetics of bromodomain complexes with AIL endecamer or histone peptide. The upper panels represent the (A) complete detachment of the AIL endecamer and (B) loss of the canonical binding mode. All the AIL endecamer iterations were pooled together. The lower panels represent (C) the complete detachment of the histone and (D) the loss of the canonical binding mode of the histone.

which was observed intramolecularly for the AIL, because they are either canonically bound or completely detached.

Kinetics of Peptide Unbinding from the Bromodomain. As with the catalytic core, we use the K1595ac distance to the structural water and a threshold of 30 Å to represent a complete unbinding event. The kinetics of AIL endecamer detachment from the bromodomain are obtained from a single-exponential fit on the cumulative distribution function (Figure 6A). The characteristic unbinding time of the AIL endecamer is about 150 ns, which is 1 order of magnitude faster than the complete detachment of the histone (about 1200 ns, Figure 6C). This result indicates that the AIL endecamer is much less stable in the CBP bromodomain binding site with respect to the histone peptide. The unbinding kinetics for each bromodomain−peptide complex are shown in Figure S2. All the AIL peptides are fit with a single-exponential function, except for the flipped AIL peptide which requires a double-exponential fit. The AIL peptides always unbind faster than the histone peptide by 1 or 2 orders of magnitude. Furthermore, we observe peptide unbinding kinetics 1 order of magnitude slower than the AIL unbinding in the catalytic core. This suggests that in solution the AIL peptide, but not the full AIL, might have a longer residence time in the bromodomain binding site.

A similar result is obtained for the unbinding of the acetylated lysine from its buried state in the pocket. Using the distance threshold of 8 Å as previously, the characteristic unbinding time is about 90 ns for the AIL endecamer (Figure 6B). The histone peptide has an unbinding time of the acetylated lysine of about 1200 ns (Figure 6D), 2 orders of magnitude slower than the K1595ac of the AIL. To validate the robustness of the acetylated lysine kinetics, we have repeated the analysis at distance thresholds between 10 and 16 Å (Table S2). The unbinding times of the K1595ac are always 1 order of magnitude faster than those of the histone; thus the analysis with a threshold of 8 Å is robust.

Contacts between the AIL Peptide and the Bromodomain. Here the contacts between the bromodomain and bound AIL peptide are analyzed. We measure all pairwise distances between the bromodomain backbone nitrogens and the heavy atoms of the bound peptide. Only the canonical and intermediate states are included, i.e., the distance of the K1595ac to the structural water up to 20 Å. The counts of the distances between backbone nitrogens and heavy atoms of the

https://doi.org/10.1021/acs.jcim.1c01423
J. Chem. Inf. Model. XXXX, XXX, XXX−XXX

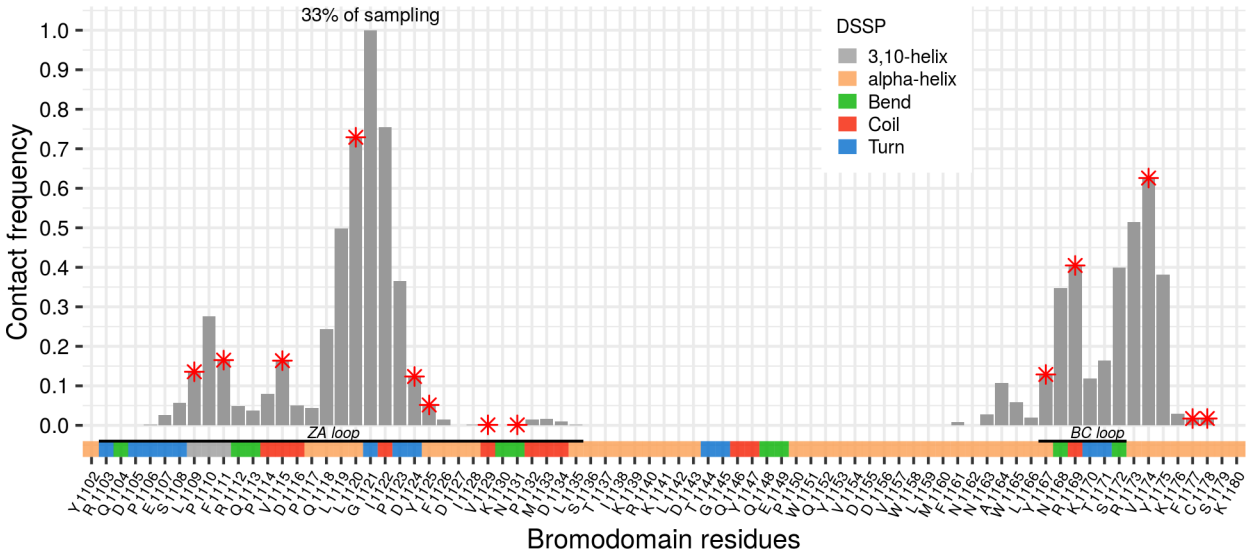

Figure 7. Contacts between the AIL endecamer and nitrogen atoms of the bromodomain. The threshold distance that defines a contact between any non-hydrogen atom of the AIL peptide and a nitrogen atom of the bromodomain backbone is 8 Å. The percentage of sampling refers to the canonical and intermediate bound states (the K1595ac distance to the structural water is below 20 Å). The red stars indicate the residues labeled in the $^{1}H-^{15}N$ HSQC spectra (Figure S6 of ref 18). The secondary structure annotation (DSSP) is shown with the color scheme in the legend.

peptide below 8 Å are summed, to have the contribution of each bromodomain residue to peptide binding. Figure 7 shows the contact frequency per residue for the AIL endecamer. Gly1121 has the highest frequency of contact (for 33% of the time that the peptide is bound to the bromodomain), because it belongs to the central and most flexible part of the ZA loop. The contacts present for 10% or more of the sampling (i.e., values of 0.3 or more in Figure 7) involve mainly hydrophobic residues, such as Leu1119, Leu1120, Ile1122, and Pro1123 of the ZA loop and Val1174 and Tyr1175 of the BC loop. As mentioned previously for the catalytic core, the hydrophobic interactions are predominant in both the canonical and intermediate states.

Our contact analysis can be compared to nuclear magnetic resonance (NMR) experiments indicating AIL peptide binding to the bromodomain,[18] which use ^{15}N-labeled CBP bromodomain with addition of the 63-residue AIL or the 7-residue AIL peptide acetylated on Lys1595 (Lys1596 in the mouse sequence used in the work). It was observed that residues with the broadest shifts of cross-peaks in the $^{1}H-^{15}N$ heteronuclear single quantum coherence (HSQC) profiles are localized on the acetylated lysine binding site, suggesting that the AIL with K1595ac might bind to the bromodomain intramolecularly. In Figure 7 we label the bromodomain residues identified as AIL peptide binders through NMR.

Many labeled residues are in agreement with our analysis, for example, Leu1120, Arg1169, and Val1174. However, we find contacts of other bromodomain residues not reported in the NMR spectra, such as Leu1119, Ile1122, Asn1168, and Arg1173, identified also in crystal structures. The partial agreement with NMR data indicates that it is possible to observe engagement of the AIL peptide to the CBP bromodomain, but the interaction is not strong enough to keep the peptide bound. Figure S3 shows the contact profile of the histone peptide calculated with the same distance thresholds. The profile is similar to the AIL endecamer, with the exception of the BC loop having more contacts. Thus, we do not identify a binding pattern unique to the AIL sequence, compared to the histone. To validate the robustness of our results with respect to the distance definition of a contact, we have repeated the analysis with threshold distances between 10 and 14 Å (Figure S4). The values of contact frequencies increase with increasing threshold distances, but the relative heights among residues remain similar. The lower threshold of 8 Å (Figure 7) is the most informative, because it includes peptide heavy atoms that are in close proximity to the backbone nitrogen atoms.

CONCLUDING DISCUSSION

The AIL of CBP/p300 is a 63-residue disordered segment which is rich in basic side chains (13 lysine residues). Its properties of intrinsically disordered region allow the AIL to regulate the acetyltransferase activity of CBP/p300. Lysine acetylation brings the AIL to switch between functional states. In the deacetylated state, the AIL occludes the HAT catalytic site, interrupting the acetyl transfer to histone tails and other proteins.[21] In the acetylated state, the AIL cannot engage with the HAT and might become a substrate for other binders, e.g., the bromodomain of the CBP/p300 catalytic core. While there is structural information on the AIL contacts with the HAT domain in p300,[20] a detailed analysis of the interactions between the AIL and the bromodomain is missing.

In this work, we have analyzed the atomic contacts and the kinetics of the AIL engagement with the bromodomain in CBP. We draw five main conclusions from the analysis of the molecular dynamics trajectories.

(i) The reconstruction of the 63-residue AIL in the CBP catalytic core reveals that a central acetylated loop lysine (K1595ac) can potentially reach the bromodomain binding pocket intramolecularly.

(ii) The bound AIL state is extremely unstable. The K1595ac of the AIL remains inserted in the bromodomain pocket for about 2 ns only. The unbinding of K1595ac is observed not only intramolecularly, but also for a noncovalent complex of the bromodomain and an 11-residue peptide derived from the AIL sequence. The complete detachment of the AIL goes through an intermediate bound state which is stabilized by hydrogen bonds between the backbone amino groups of K1595ac and Asn1596 and the carbonyl of Leu1120, while the acetyl moiety of K1595ac is solvent exposed.

https://doi.org/10.1021/acs.jcim.1c01423
J. Chem. Inf. Model. XXXX, XXX, XXX−XXX

(iii) The intramolecular unbinding kinetics of the AIL are at least 1 order of magnitude faster than those of the AIL peptides. Thus, while it is possible to observe intermolecular binding of AIL peptides to the bromodomain in solution,[18] the AIL intramolecular binding to the bromodomain is less likely in the context of the CBP catalytic core. It is important to note here that, although any simulation is based on simplified models, the approximations inherent to the (any) implicit model of the solvent have a smaller influence on relative unbinding kinetics than absolute ones.

(iv) From the analysis of contacts at the interface, the main contributions to AIL binding come from nonpolar contacts, given the hydrophobicity of the ZA loop, and backbone hydrogen bonds, which are independent of the AIL sequence. The absence of persistent hydrogen bonds with the AIL side chains suggests that the AIL sequence does not engage the bromodomain in a unique binding mode. The contact analysis from MD simulations reveals a pattern of interactions between the bromodomain and the AIL peptide similar to the one identified with NMR spectroscopy.[18] While the $^{1}H-^{15}N$ HSQC spectrum identifies a limited number of bromodomain residues contacting the AIL peptide, our analysis adds quantitative information on the contacts between all bromodomain residues and the AIL endecamer.

(v) The MD simulations of a control histone peptide in the bromodomain validate our analysis. The histone detachment is always 1 or 2 orders of magnitude slower than that of the AIL peptide, which provides evidence that it is more stable in the bromodomain pocket.

In our study, we have focused on a single acetylation mark of the AIL, to have a direct comparison with the results from NMR.[18] The acetylation of all AIL lysines is expected to influence the dynamics of the loop, and it remains to be investigated if multiple acetylation marks on the AIL would improve the interactions with the bromodomain pocket. However, we did not identify persistent contacts between the AIL lysines and the bromodomain, so it is likely that further acetylation would not result in a significant occupancy of the bromodomain pocket by the tip of the AIL. Furthermore, it will be interesting to verify if similar conclusions can be drawn for p300. Unbinding of the AIL in p300 is a likely hypothesis, given the sequence similarity of the two proteins and the conserved catalytic core structure. In agreement with our simulation results for the AIL of CBP, Panne and co-workers reported a lack of binding between triacetylated AIL peptides and the p300 bromodomain according to isothermal titration calorimetry measurements.[20] In conclusion, the simulation results indicate that the AIL of CBP cannot form favorable intramolecular interactions with the acetyl-lysine recognition pocket of the bromodomain.

MATERIALS AND METHODS

Reconstruction of the Missing AIL. The stretch of 63 residues (1556−1618 in the human CBP sequence) corresponding to the missing AIL was added to the crystal structure of the CBP catalytic core (PDB 5U7G) with MODELLER.[49] The system contains 620 residues, including the reconstructed loop. As the crystal was obtained with the mouse sequence of CBP, we have mutated the residues to the human CBP sequence. The mouse and human orthologs differ by few residues, as shown in the sequence alignment in Figure S5. The lysine at position 1595 in human CBP was chosen for acetylation (called K1595ac), to compare our results to previous NMR data.[18] Using a harmonic potential function, we have restrained the distances between K1595ac and specific residues in the bromodomain, to insert the K1595ac into the binding pocket. The analysis of contacts from the available crystal structures of the CBP bromodomain with histone peptides allowed generation of the optimal position of the K1595ac in the bromodomain pocket. Importantly, there are structural water molecules that are always present in the crystal structures and are crucial to acetylated lysine binding.[48,50,51] We have added one explicit water molecule to bridge the hydrogen bond between the acetyl moiety of K1595ac and the Tyr1125 of the bromodomain ZA loop (an interaction conserved among bromodomains).

Molecular Dynamics Simulations. We have carried out MD simulations of the catalytic core and of the CBP bromodomain in complex with the AIL peptides and the histone peptide. Each system was simulated in 36 replicas with identical settings but different atomic velocities at the start. We used the simulation software CAMPARI (http://campari.sourceforge.net/V4/) with the CHARMM36 force field[52] and the ABSINTH implicit solvent model.[53] We employed torsional molecular dynamics which samples conformations of freely rotatable dihedral angles.[54] We used a spherical droplet of solvent (implicit treatment of water and explicit ions), with a radius of 200 Å for the CBP catalytic core and 100 Å for the CBP bromodomain. The catalytic core system has one negative ion (Cl^-) necessary to neutralize the overall charge. The bromodomain−AIL peptide complex has one positive counterion (K^+), and the bromodomain−histone complex has three positive counterions (K^+). All polypeptide chains were capped with an acetyl group (Ace) and a methylamide group (Nme) at the N- and C-terminals, respectively. The flexible regions of the simulation system are indicated in Table 3. All other segments were kept rigid. The flexible segments are indicated in red on the structure in Figure S1. To maintain the explicit structural water in place, the following three distances from its oxygen atom were restrained with a harmonic potential: distance to the Tyr1125-(OH) ≤3 Å; distance to the Met1180(O) ≤5 Å; distance to the Asn1183(O) ≤6 Å. The harmonic restraints are necessary because in implicit solvent the effect of bulk water (e.g., network of hydrogen bonds and exchange between water molecules) is not possible, and the single water molecule would drift away from the binding site. The distance restraint between the water oxygen and the K1595ac(acetyl O) of ≤3 Å was used only during the equilibration phase, to keep the AIL bound. The CBP catalytic core was equilibrated for 40 ns. The first 4 ns were discarded, and 36 structures sampled at 1 ns intervals were chosen to start the 36 production runs. The trajectories were analyzed with GROMACS and CAMPARI. Calculations and final plots were generated with R.[55] Structures and trajectories were visualized with VMD.[56]

Table 3. Flexible Components of the Solute during Simulations

side chains of all residues
backbone of AIL (residues 1556−1618)
backbone of bromodomain loops (residues 1103−1135 and 1167−1172)
backbone of hinges (residues 1197−1279, 1316−1322, and 1537−1543)

Data and Software Availability. The CAMPARI software necessary for running the MD simulations is publicly available at http://campari.sourceforge.net/V4/. Usage instructions and documentation are provided. The complete MD trajectories

https://doi.org/10.1021/acs.jcim.1c01423
J. Chem. Inf. Model. XXXX, XXX, XXX−XXX

and the R scripts used (a) to plot the RMSD time series, (b) to plot the distance distributions, (c) to plot the contact maps, (d) to calculate the unbinding kinetics, and (e) to plot the bromodomain nitrogen−peptide distances are available from the author upon request.

■ ASSOCIATED CONTENT

Supporting Information

The Supporting Information is available free of charge at https://pubs.acs.org/doi/10.1021/acs.jcim.1c01423.

Characteristic unbinding times of K1595ac from the bromodomain in the catalytic core and of acetylated lysine in bromodomain complexes with AIL endecamer and histone peptide; overlap of CBP crystal structure 5U7G and equilibrated model of CBP catalytic core; time series of RMSD of bromodomain α-helices after fitting to the HAT domain of the crystal structure; kinetics of complete peptide unbinding in all bromodomain−peptide complexes; contact analysis between bromodomain backbone nitrogen atoms and all heavy atoms of the histone peptide and the AIL endecamer; alignment of CBP catalytic core sequences from human and mouse organisms (PDF)

■ AUTHOR INFORMATION

Corresponding Author

Amedeo Caflisch − *Department of Biochemistry, University of Zürich, CH-8057 Zürich, Switzerland;* orcid.org/0000-0002-2317-6792; Phone: 41-44-635-5568; Email: caflisch@bioc.uzh.ch

Author

Ilaria Salutari − *Department of Biochemistry, University of Zürich, CH-8057 Zürich, Switzerland;* orcid.org/0000-0002-4644-9538

Complete contact information is available at: https://pubs.acs.org/10.1021/acs.jcim.1c01423

Notes

The authors declare no competing financial interest.

■ ACKNOWLEDGMENTS

We thank Cassiano Langini for interesting discussions. This work was supported financially by an excellence grant of the Swiss National Science Foundation (310030B-189363) to A.C.

■ REFERENCES

(1) Neely, K. E.; Workman, J. L. Histone acetylation and chromatin remodeling: which comes first? *Mol. Genet. Metab.* **2002**, *76*, 1−5.

(2) Roth, S. Y.; Denu, J. M.; Allis, C. D. Histone Acetyltransferases. *Annu. Rev. Biochem.* **2001**, *70*, 81−120.

(3) Yang, X. J.; Seto, E. HATs and HDACs: From structure, function and regulation to novel strategies for therapy and prevention. *Oncogene* **2007**, *26*, 5310−5318.

(4) Kouzarides, T. Chromatin modifications and their function. *Cell* **2007**, *128*, 693−705.

(5) Bannister, A. J.; Kouzarides, T. The CBP co-activator is a histone acetyltransferase. *Nature 1996 384:6610* **1996**, *384*, 641−643.

(6) Bedford, D. C.; Kasper, L. H.; Fukuyama, T.; Brindle, P. K. Target gene context influences the transcriptional requirement for the KAT3 family of CBP and p300 histone acetyltransferases. *Epigenetics* **2010**, *5*, 9−15.

(7) Ramos, Y. F. M.; Hestand, M. S.; Verlaan, M.; Krabbendam, E.; Ariyurek, Y.; van Galen, M.; van Dam, H.; van Ommen, G.-J. B.; den Dunnen, J. T.; Zantema, A.; 't Hoen, P. A. C. Genome-wide assessment of differential roles for p300 and CBP in transcription regulation. *Nucleic acids research* **2010**, *38*, 5396−5408.

(8) Tanaka, Y.; Naruse, I.; Maekawa, T.; Masuya, H.; Shiroishi, T.; Ishii, S. Abnormal skeletal patterning in embryos lacking a single Cbp allele: a partial similarity with Rubinstein−Taybi syndrome. *Proc. Natl. Acad. Sci. U. S. A.* **1997**, *94*, 10215−10220.

(9) Yao, T.-P.; Oh, S. P.; Fuchs, M.; Zhou, N.-D.; Ch'ng, L.-E.; Newsome, D.; Bronson, R. T.; Li, E.; Livingston, D. M.; Eckner, R. Gene dosage-dependent embryonic development and proliferation defects in mice lacking the transcriptional integrator p300. *Cell* **1998**, *93*, 361−372.

(10) Kung, A. L.; Rebel, V. I.; Bronson, R. T.; Ch'ng, L.-E.; Sieff, C. A.; Livingston, D. M.; Yao, T.-P. Gene dose-dependent control of hematopoiesis and hematologic tumor suppression by CBP. *Genes Dev.* **2000**, *14*, 272−277.

(11) Roelfsema, J. H.; White, S. J.; Ariyürek, Y.; Bartholdi, D.; Niedrist, D.; Papadia, F.; Bacino, C. A.; Den Dunnen, J. T.; Van Ommen, G. J. B.; Breuning, M. H.; Hennekam, R. C.; Peters, D. J. Genetic heterogeneity in Rubinstein-Taybi syndrome: mutations in both the CBP and EP300 genes cause disease. *American Journal of Human Genetics* **2005**, *76*, 572−580.

(12) Kasper, L. H.; Fukuyama, T.; Biesen, M. A.; Boussouar, F.; Tong, C.; de Pauw, A.; Murray, P. J.; van Deursen, J. M. A.; Brindle, P. K. Conditional knockout mice reveal distinct functions for the global transcriptional coactivators CBP and p300 in T-Cell development. *Mol. Cell. Biol.* **2006**, *26*, 789−809.

(13) Chakravarti, D.; Ogryzko, V.; Kao, H.-Y.; Nash, A.; Chen, H.; Nakatani, Y.; Evans, R. M. A viral mechanism for inhibition of p300 and PCAF acetyltransferase activity. *Cell* **1999**, *96*, 393−403.

(14) Hamamori, Y.; Sartorelli, V.; Ogryzko, V.; Puri, P. L.; Wu, H. Y.; Wang, J. Y.; Nakatani, Y.; Kedes, L. Regulation of histone acetyltransferases p300 and PCAF by the bHLH protein Twist and adenoviral oncoprotein E1A. *Cell* **1999**, *96*, 405−413.

(15) Saint Just Ribeiro, M.; Hansson, M. L.; Wallberg, A. E. A proline repeat domain in the Notch co-activator MAML1 is important for the p300-mediated acetylation of MAML1. *Biochemical journal* **2007**, *404*, 289−298.

(16) Mukherjee, S. P.; Behar, M.; Birnbaum, H. A.; Hoffmann, A.; Wright, P. E.; Ghosh, G. Analysis of the RelA:CBP/p300 interaction reveals its involvement in NF-κB-driven transcription. *PLOS Biology* **2013**, *11*, e1001647.

(17) Diehl, C.; Akke, M.; Bekker-Jensen, S.; Mailand, N.; Streicher, W.; Wikström, M. Structural analysis of a complex between Small Ubiquitin-like Modifier 1 (SUMO1) and the ZZ domain of CREB-Binding Protein (CBP/p300) reveals a new interaction surface on SUMO. *J. Biol. Chem.* **2016**, *291*, 12658−12672.

(18) Park, S.; Stanfield, R. L.; Martinez-Yamout, M. A.; Dyson, H. J.; Wilson, I. A.; Wright, P. E. Role of the CBP catalytic core in intramolecular SUMOylation and control of histone H3 acetylation. *Proc. Natl. Acad. Sci. U. S. A.* **2017**, *114*, E5335−E5342.

(19) Delvecchio, M.; Gaucher, J.; Aguilar-Gurrieri, C.; Ortega, E.; Panne, D. Structure of the p300 catalytic core and implications for chromatin targeting and HAT regulation. *Nature Structural & Molecular Biology* **2013**, *20*, 1040−1046.

(20) Ortega, E.; Rengachari, S.; Ibrahim, Z.; Hoghoughi, N.; Gaucher, J.; Holehouse, A. S.; Khochbin, S.; Panne, D. Transcription factor dimerization activates the p300 acetyltransferase. *Nature* **2018**, *562*, 538−544.

(21) Thompson, P. R.; Wang, D.; Wang, L.; Fulco, M.; Pediconi, N.; Zhang, D.; An, W.; Ge, Q.; Roeder, R. G.; Wong, J.; Levrero, M.; Sartorelli, V.; Cotter, R. J.; Cole, P. A. Regulation of the p300 HAT domain via a novel activation loop. *Nature Structural & Molecular Biology* **2004**, *11*, 308−315.

(22) Liu, X.; Wang, L.; Zhao, K.; Thompson, P. R.; Hwang, Y.; Marmorstein, R.; Cole, P. A. The structural basis of protein acetylation by the p300/CBP transcriptional coactivator. *Nature* **2008**, *451*, 846−850.

(23) Filippakopoulos, P.; Picaud, S.; Mangos, M.; Keates, T.; Lambert, J.-P.; Barsyte-Lovejoy, D.; Felletar, I.; Volkmer, R.; Müller, S.; Pawson,

T.; Gingras, A.-C.; Arrowsmith, C.; Knapp, S. Histone recognition and large-scale structural analysis of the human bromodomain family. *Cell* **2012**, *149*, 214−231.
(24) Steiner, S.; Magno, A.; Huang, D.; Caflisch, A. Does bromodomain flexibility influence histone recognition? *FEBS Lett.* **2013**, *587*, 2158−2163.
(25) Zhang, X.; Chen, K.; Wu, Y.-D.; Wiest, O. Protein dynamics and structural waters in bromodomains. *PLoS One* **2017**, *12*, e0186570.
(26) Bacci, M.; Langini, C.; Vymětal, J.; Caflisch, A.; Vitalis, A. Focused conformational sampling in proteins. *J. Chem. Phys.* **2017**, *147*, 195102.
(27) Zhou, Y.; Hussain, M.; Kuang, G.; Zhang, J.; Tu, Y. Mechanistic insights into peptide and ligand binding of the ATAD2-bromodomain via atomistic simulations disclosing a role of induced fit and conformational selection. *Phys. Chem. Chem. Phys.* **2018**, *20*, 23222−23232.
(28) Raich, L.; Meier, K.; Günther, J.; Christ, C. D.; Noé, F.; Olsson, S. Discovery of a hidden transient state in all bromodomain families. *Proc. Natl. Acad. Sci. U. S. A.* **2021**, *118*, e2017427118.
(29) Pizzitutti, F.; Giansanti, A.; Ballario, P.; Ornaghi, P.; Torreri, P.; Ciccotti, G.; Filetici, P. The role of loop ZA and Pro371 in the function of yeast Gcn5p bromodomain revealed through molecular dynamics and experiment. *Journal of Molecular Recognition* **2006**, *19*, 1−9.
(30) Eichenbaum, K. D.; Rodríguez, Y.; Mezei, M.; Osman, R. The energetics of the acetylation switch in p53-mediated transcriptional activation. *Proteins* **2010**, *78*, 447−456.
(31) Magno, A.; Steiner, S.; Caflisch, A. Mechanism and kinetics of acetyl-lysine binding to bromodomains. *J. Chem. Theory Comput.* **2013**, *9*, 4225−4232.
(32) Spiliotopoulos, D.; Caflisch, A. Molecular dynamics simulations of bromodomains reveal binding-site flexibility and multiple binding modes of the natural ligand acetyl-lysine. *Isr. J. Chem.* **2014**, *54*, 1084−1092.
(33) Langini, C.; Caflisch, A.; Vitalis, A. The ATAD2 bromodomain binds different acetylation marks on the histone H4 in similar fuzzy complexes. *J. Biol. Chem.* **2017**, *292*, 16734−16745.
(34) Barman, S.; Roy, A.; Bardhan, I.; Kandasamy, T.; Shivani, S.; Sudhamalla, B. Insights into the molecular mechanisms of histone code recognition by the BRPF3 bromodomain. *Chemistry - An Asian Journal* **2021**, *16*, 3404−3412.
(35) Ran, T.; Zhang, Z.; Liu, K.; Lu, Y.; Li, H.; Xu, J.; Xiong, X.; Zhang, Y.; Xu, A.; Lu, S.; Liu, H.; Lu, T.; Chen, Y. Insight into the key interactions of bromodomain inhibitors based on molecular docking, interaction fingerprinting, molecular dynamics and binding free energy calculation. *Molecular BioSystems* **2015**, *11*, 1295−1304.
(36) Xu, M.; Unzue, A.; Dong, J.; Spiliotopoulos, D.; Nevado, C.; Caflisch, A. Discovery of CREBBP bromodomain inhibitors by high-throughput docking and hit optimization guided by molecular dynamics. *J. Med. Chem.* **2016**, *59*, 1340−1349.
(37) Śledź, P.; Caflisch, A. Protein structure-based drug design: from docking to molecular dynamics. *Curr. Opin. Struct. Biol.* **2018**, *48*, 93−102.
(38) Su, J.; Liu, X.; Zhang, S.; Yan, F.; Zhang, Q.; Chen, J. A theoretical insight into selectivity of inhibitors toward two domains of bromodomain-containing protein 4 using molecular dynamics simulations. *Chemical Biology & Drug Design* **2018**, *91*, 828−840.
(39) Su, J.; Liu, X.; Zhang, S.; Yan, F.; Zhang, Q.; Chen, J. Insight into selective mechanism of class of I-BRD9 inhibitors toward BRD9 based on molecular dynamics simulations. *Chemical Biology & Drug Design* **2019**, *93*, 163−176.
(40) Dolbois, A.; Batiste, L.; Wiedmer, L.; Dong, J.; Brütsch, M.; Huang, D.; Deerain, N. M.; Spiliotopoulos, D.; Cheng-Sánchez, I.; Laul, E.; Nevado, C.; Śledź, P.; Caflisch, A. Hitting a moving target: simulation and crystallography study of ATAD2 bromodomain blockers. *ACS Med. Chem. Lett.* **2020**, *11*, 1573−1580.
(41) Xu, L.; Cheng, A.; Huang, M.; Zhang, J.; Jiang, Y.; Wang, C.; Li, F.; Bao, H.; Gao, J.; Wang, N.; Liu, J.; Wu, J.; Wong, C. C.; Ruan, K. Structural insight into the recognition of acetylated histone H3K56ac mediated by the bromodomain of CREB-binding protein. *FEBS Journal* **2017**, *284*, 3422−3436.
(42) Owen, D. J.; Ornaghi, P.; Yang, J. C.; Lowe, N.; Evans, P. R.; Ballario, P.; Neuhaus, D.; Filetici, P.; Travers, A. A. The structural basis for the recognition of acetylated histone H4 by the bromodomain of histone acetyltransferase Gcn5p. *EMBO journal* **2000**, *19*, 6141−6149.
(43) Huang, D.; Caflisch, A. Small molecule binding to proteins: affinity and binding/unbinding dynamics from atomistic simulations. *ChemMedChem.* **2011**, *6*, 1578−1580.
(44) Plotnikov, A. N.; Yang, S.; Zhou, T.; Rusinova, E.; Frasca, A.; Zhou, M.-M. Structural insights into acetylated-histone H4 recognition by the bromodomain-PHD finger module of human transcriptional coactivator CBP. *Structure* **2014**, *22*, 353−360.
(45) Zhang, Q.; Chakravarty, S.; Ghersi, D.; Zeng, L.; Plotnikov, A. N.; Sanchez, R.; Zhou, M.-M. Biochemical profiling of histone binding selectivity of the yeast bromodomain family. *PLoS One* **2010**, *5*, e8903.
(46) *The PyMOL Molecular Graphics System*, ver. 1.8; Schrödinger, LLC: 2015.
(47) Ruthenburg, A. J.; Li, H.; Milne, T. A.; Dewell, S.; McGinty, R. K.; Yuen, M.; Ueberheide, B.; Dou, Y.; Muir, T. W.; Patel, D. J.; Allis, C. D. Recognition of a mononucleosomal histone modification pattern by BPTF via multivalent interactions. *Cell* **2011**, *145*, 692−706.
(48) Marchand, J. R.; Caflisch, A. Binding mode of acetylated histones to bromodomains: variations on a common motif. *ChemMedChem.* **2015**, *10*, 1327−1333.
(49) Šali, A.; Blundell, T. L. Comparative protein modelling by satisfaction of spatial restraints. *J. Mol. Biol.* **1993**, *234*, 779−815.
(50) Hewings, D. S.; Rooney, T. P. C.; Jennings, L. E.; Hay, D. A.; Schofield, C. J.; Brennan, P. E.; Knapp, S.; Conway, S. J. Progress in the development and application of small molecule inhibitors of bromodomain-acetyl-lysine interactions. *J. Med. Chem.* **2012**, *55*, 9393−9413.
(51) Huang, D.; Rossini, E.; Steiner, S.; Caflisch, A. Structured water molecules in the binding site of bromodomains can be displaced by cosolvent. *ChemMedChem.* **2014**, *9*, 573−579.
(52) Best, R. B.; Zhu, X.; Shim, J.; Lopes, P. E. M.; Mittal, J.; Feig, M.; MacKerell, A. D. Optimization of the additive CHARMM all-atom protein force field targeting improved sampling of the backbone ϕ, ψ and side-Chain χ_1 and χ_2 dihedral angles. *J. Chem. Theory Comput.* **2012**, *8*, 3257−3273.
(53) Vitalis, A.; Pappu, R. V. ABSINTH: A new continuum solvation model for simulations of polypeptides in aqueous solutions. *J. Comput. Chem.* **2009**, *30*, 673−699.
(54) Vitalis, A.; Pappu, R. V. A simple molecular mechanics integrator in mixed rigid body and dihedral angle space. *J. Chem. Phys.* **2014**, *141*, No. 034105.
(55) R Core Team. *R: A Language and Environment for Statistical Computing*; R Foundation for Statistical Computing: 2014.
(56) Humphrey, W.; Dalke, A.; Schulten, K. VMD − Visual Molecular Dynamics. *J. Mol. Graphics* **1996**, *14*, 33−38.

https://doi.org/10.1021/acs.jcim.1c01423
J. Chem. Inf. Model. XXXX, XXX, XXX−XXX